Letter

Universal Kardar-Parisi-Zhang scaling in noisy hybrid quantum circuits

Shuo Liu,[1,*] Ming-Rui Li,[1,*] Shi-Xin Zhang,[2,†] Shao-Kai Jian,[3,‡] and Hong Yao[1,§]
[1]*Institute for Advanced Study, Tsinghua University, Beijing 100084, China*
[2]*Tencent Quantum Laboratory, Tencent, Shenzhen, Guangdong 518057, China*
[3]*Department of Physics and Engineering Physics, Tulane University, New Orleans, Louisiana, 70118, USA*

(Received 2 January 2023; accepted 5 May 2023; published 22 May 2023)

Measurement-induced phase transitions (MIPTs) have attracted increasing attention due to the rich phenomenology of entanglement structures and their relation with quantum information processing. Since physical systems are unavoidably coupled to environment, quantum noise, which can qualitatively modify or even destroy certain entanglement structure, needs to be considered in analyzing a system with MIPT. In this Letter, we investigate the effect of quantum noise modeled by a reset quantum channel acting on each site with a probability q on MIPT. Based on the numerical results from Clifford circuits, we show that the quantum noise can qualitatively change the entanglement properties—the entanglement obeys "area law" instead of "volume law" with a measurement rate $p < p_c$. In the noise-induced area law phase, the entanglement exhibits a novel $q^{-1/3}$ power-law scaling. Using an analytic mapping from the quantum model to a classical statistical model, we further show that the area law entanglement is the consequence of noise-driven symmetry-breaking field, and the $q^{-1/3}$ scaling can be understood as the result of Kardar-Parisi-Zhang fluctuations of directed polymer with an effective length scale $L_{\text{eff}} \sim q^{-1}$ in a random environment.

DOI: 10.1103/PhysRevB.107.L201113

Introduction. The monitored quantum systems undergoing random unitary evolution interspersed by local measurements can present rich entanglement structures. The random unitary evolution generates entanglement within the system whereas the monitored measurement tends to render the system short-range entangled. The competition between unitary evolution and monitored measurement leads to the measurement-induced phase transitions [1–14]. Below a critical measurement rate p_c, the system exhibits large-scale quantum entanglement as the "volume law" entanglement phase. Increasing the measurement rate p above the critical rate, the effect of measurements dominates, and the entanglement obeys "area law." The measurement-induced phase transition has also been investigated in the monitored Sachdev—Ye—Kitaev models [15–17], the classical single random walker [18], and the monitored systems with long-range interactions [8,15,19–28].

Real physical systems are unavoidably coupled to an environment and, thus, evolve into mixed states in which von Neumann entropy fails to quantify the quantum entanglement [29,30] whereas the logarithmic entanglement negativity is still a good measure for the mixed-state bipartite entanglement [31–41]. The quantum noise and decoherence, induced by the environment can suppress entanglement within the systems and are the major obstacles in quantum information processing [1,3,42–48]. As known before [49–51], the bulk quantum noises drive the systems to enter the area law entanglement phase instead of the volume law phase below the MIPT, which can be understood as a consequence of the symmetry-breaking field in an effective statistical model. Nevertheless, there is a power-law scaling in terms of the system size for the entanglement in the presence of fixed dephasing quantum noise at the spatial boundary [52]. A straightforward and vital question is whether there is a unified analytic model to understand the effect of quantum noises of different types and with different space-time distributions in hybrid circuits.

Despite the similarity of different quantum channels in the large-d limit of the classical statistical model, their effects remain to be investigated in the quantum system with qubits (with local Hilbert space dimension $d = 2$), which are more relevant for experimental implementation of MIPT [53]. Besides the dephasing channel, reset operation can also model the uncontrolled quantum noise in which the lth qubit is reset to the $|0\rangle$ state by the reset quantum channel R_l. In addition, the reset channel is easy to implement in the current generation of quantum hardware, which is of great experimental relevance as a controllable noise source [54,55].

In this Letter, we investigate the entanglement behaviors of a monitored system in the presence of quantum noise modeled by reset quantum channels. We focus on the case when the probability of measurement p is nonzero and below the critical probability p_c where the system sustains large-scale entanglement in the absence of quantum noise. See the Supplemental Material (SM) [56] (see also Refs. [57–66] therein) for discussions with $p > p_c$ and $p = 0$. To quantify the entanglement of the mixed state, we investigate the logarithmic entanglement negativity E_N as well as the mutual information $I_{A:B}$ which has similar qualitative properties as the logarithmic entanglement negativity.

*These authors contributed equally to this work.
†shixinzhang@tencent.com
‡sjian@tulane.edu
§yaohong@tsinghua.edu.cn

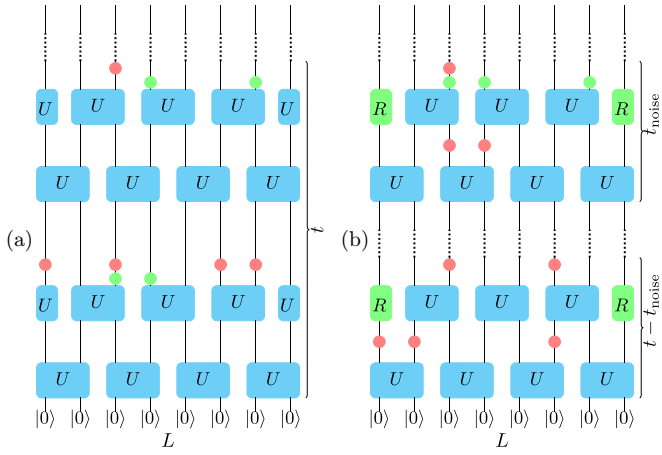

FIG. 1. (a) Circuit diagram in the presence of random bulk resets with $L = 8$ qudits and periodic boundary conditions (PBCs). Qudits are initialized to the product state $|0\rangle^L$ and evolved by applying random two-qudit Clifford gates (blue blocks). Projective measurements (red dots) and reset quantum channels (green dots) occur randomly at rates p and q, respectively. (b) Circuit diagram in the presence of fixed resets at the spatial boundary (green blocks) with $L = 8$ qudits. On the last $t_{\rm noise}$ time steps, the reset quantum channels (green dots) occur randomly at a rate q in the bulk. We set $t = 8L$ throughout the Letter to observe the late-time properties.

In the presence of random bulk resets with an occurring probability q [see Fig. 1(a)], the entanglement obeys area law as predicted by the previous studies [50]. Besides, we report a novel power-law scaling for entanglement in terms of the reset probability q, $I_{A:B}(q) \sim q^{-1/3}$ and $E_N(q) \sim q^{-1/3}$. To deepen our understanding, we map the random quantum circuit to an effective statistical model [52]. Intuitively, the mutual information and logarithmic entanglement negativity can be interpreted as the free-energy difference of the statistical models with different boundary conditions and is proportional to the length of the domain wall, which can be mapped to a directed polymer in a random potential induced by the randomness of measurement locations. The bulk resets act as a symmetry-breaking field that suppresses the vertical fluctuations of the directed polymer and drives the system into an area law entanglement phase. The resets near the top temporal boundary induce an effective length scale $L_{\rm eff} \sim q^{-1}$, and the novel $q^{-1/3}$ scaling for entanglement can be understood as the result of Kardar-Paris-Zhang (KPZ) fluctuations of domain walls [67–69] with the effective length scale $L_{\rm eff}$ instead of the original length scale L [56]. It is worth noting that the existence of measurement, which acts as random potential in the statistical model is necessary for the application of KPZ field theory. Therefore, $q^{-1/3}$ scaling disappears for the zero measurement case [56].

Furthermore, such an analytic model can unify the models with quantum noise at the spatial boundary and in the bulk. To verify this analytic model, we also investigate the entanglement behaviors for the system with fixed resets at the spatial boundary and random bulk resets on the last $t_{\rm noise}$ layers with rate q, see Fig. 1(b). When $t_{\rm noise} = 0$, it exhibits $L^{1/3}$ power-law entanglement [52] induced by KPZ fluctuations of the original length scale L as shown in the lower panel of Fig. 3. Via increasing $t_{\rm noise}$, i.e., the strength of quantum noise, the entanglement is suppressed, and the system enters the area law phase. In this noise-driven area law phase, the $q^{-1/3}$ scaling emerges with an effective length scale $L_{\rm eff}$ as shown in the upper panel of Fig. 3. In the $t_{\rm noise} \to \infty$ limit, the model is equivalent to the one in Fig. 1(a) and the $q^{-1/3}$ scaling remains. Based on the analytical understanding, the entanglement behaviors can be unified as $L_{\rm eff}^{1/3}$, where different space-time distributions of quantum noise set different $L_{\rm eff}$'s.

Model and observables. As indicated in Fig. 1(a), we investigate a one-dimensional system with L d-qudits with initial input state $|0\rangle^L$. The evolution of the system is determined by a brick-wall random unitary circuit with PBCs where each gate is independently drawn from the Haar ensemble (or from the random two-qubit Clifford ensemble in Clifford simulation). Each single discrete time step consists of four layers. The first two layers are the Haar random unitary two-qudit gates, followed by one layer of reset quantum channels occurring at a rate q on each site l and one layer of projective measurements occurring at a rate p on each site l'. The reset quantum channel R_l on the lth qudit takes the density matrix ρ to the mixed state,

$$\rho' = R_l[\rho] = \sum_{a=0}^{d-1} E_l^a \rho E_l^{a\dagger}, \tag{1}$$

where the Kraus operator $E_l^{a\dagger} = |a\rangle_l\langle 0|$. The projective measurement on the l'th qubit take the density-matrix ρ to $P_{l'}^a \rho P_{l'}^{a\dagger}/\|P_{l'}^a \rho P_{l'}^{a\dagger}\|$ with probability $p_a = \|P_{l'}^a \rho P_{l'}^{a\dagger}\|$ for $a = 0, 1, \ldots, d-1$, where $P_{l'}^{a\dagger} = P_{l'}^a = |a\rangle_{l'}\langle a|$.

The quantum entanglement at late times ($t = 8L$) is quantified by the logarithmic entanglement negativity,

$$E_N = \log\|\rho^{T_B}\|_1, \tag{2}$$

where ρ^{T_B} is the partial transpose of ρ in subsystem B and $\|\cdot\|_1$ is the trace norm. E_N is a measure of mixed-state bipartite entanglement [31–40] where entanglement entropy fails [29,30]. The mutual information obeys qualitatively similar scaling to E_N and is more intuitive as shown below. The mutual information between subsystems A and B is given by

$$I_{A:B} = S_A + S_B - S_{AB}, \tag{3}$$

where S_α is the von Neumann entropy ($\alpha = A, B, AB$). We set subsystem $A = [0, L/2]$ and $B = [L/2, L]$ throughout the work.

Numerical results with bulk resets. To avoid the severe finite-size effects, we employ random Clifford unitary gates acting on $d = 2$ qubits which can be simulated efficiently based on the stabilizer formalism. The Clifford gates form a unitary three-designs [70,71] and, thus, are expected to give the same qualitative entanglement behaviors as the Haar random circuit. And the entanglement in the thermodynamic limit $L \to \infty$ can be extrapolated by assuming $S(L, q) = c(q)L^{-1} + S(\infty, q)$ (S is $I_{A:B}$ or E_N) [20,72].

For the monitored systems shown in Fig. 1(a) without resets, i.e., $q = 0$, the critical measurement rate is $0.30 < p_c < 0.31$ [50]. Below the critical measurement rate p_c, the entanglement within the system obeys volume law, i.e., $I_{A:B}(L) \sim L$ and $E_N(L) \sim L$ as shown in the insets of Fig. 2. With

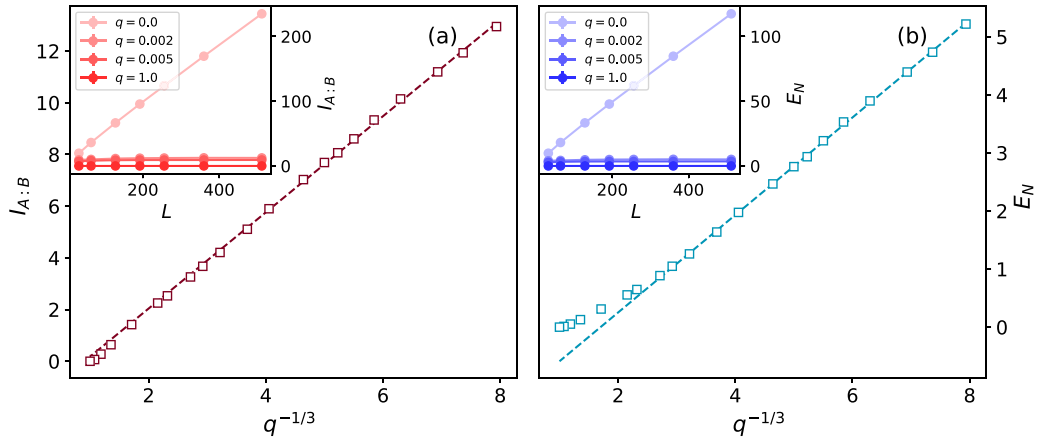

FIG. 2. (a) $I_{A:B}(q)$ and (b) $E_N(q)$ with PBC. The measurement rate is $p = 0.1 < p_c$. There is a novel $q^{-1/3}$ scaling for the entanglement within the system. The inset is the relationship between $I_{A:B}$ or E_N and the system size L with different reset rates. In the absence of resets, the entanglement obeys the volume law; in the presence of resets, the entanglement obeys the area law. As q is close to 1, the entanglement deviates from the predicted value from $q^{-1/3}$ scaling, which can be explained as the breakdown of KPZ field theory due to the small effective length scale.

increasing the measurement rate p above p_c, the system enters the area law entanglement phase, i.e., $I_{A:B}(L) \sim L^0$ and $E_N(L) \sim L^0$. When the quantum noises modeled by reset channels are added into the circuit with probability q, we focus on the case with $0 < p < p_c$ and set $p = 0.1$, which is deep in the original volume law phase (see Ref. [56] for more details). There is a novel power-law scaling in terms of q: $I_{A:B}(q) \sim q^{-1/3}$ and $E_N(q) \sim q^{-1/3}$, besides the expected area law entanglement phase in terms of the system size as indicated in Fig. 2. The emergent $q^{-1/3}$ scaling can be understood as the consequence of the KPZ fluctuations with an effective length scale $L_{\text{eff}} \sim q^{-1}$ as discussed below [56].

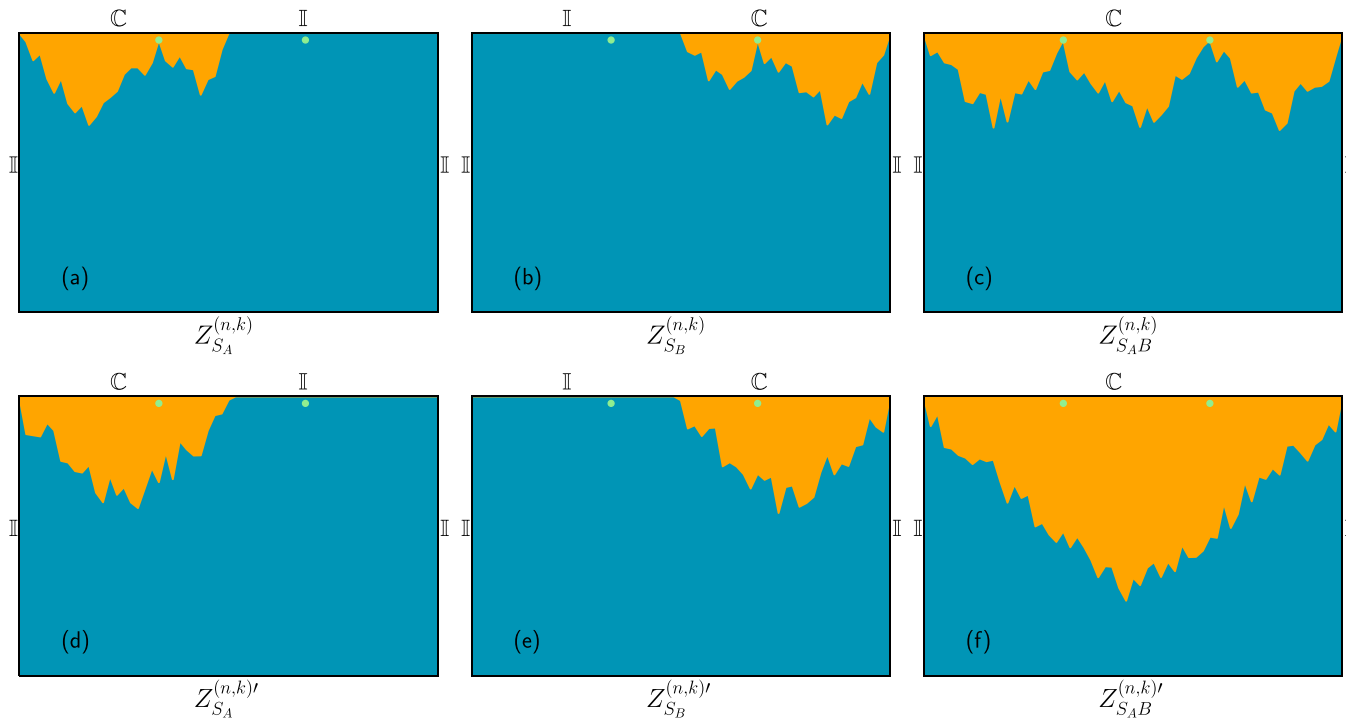

FIG. 3. Two possible scenarios for domain configuration in the presence of resets. x axis and y axis correspond to space and time dimensions in the original quantum circuit. The three subfigures in a row represent the most probable configuration for S_A, S_B, and S_{AB}, respectively. The resets near the top boundary are represented by green dots and the resets in the bulk are not shown. The domain configurations with effective length scale q^{-1} as shown in (a)–(c) minimize the free energy as much fewer bulk reset channels are contained in the region between the upper boundary and domain wall (indicated by yellow color). This is in contrast with the domain configurations where the KPZ length scale is L, as shown in (d)–(f). Namely, the first row corresponds to the realistic scenario based on the free-energy minimization principle. Due to the ferromagnetic spin-spin interaction and symmetry-breaking fields induced by resets, the domain below the domain wall (indicated by the blue color) always favors identity permutation.

When $q = 1$, the steady state is exactly the product state $|0\rangle^L$ and $I_{A:B} = E_N = 0$ as shown in Fig. 2. As q is close to 1 and, thus, the effective length scale is of the same order as the discrete lattice constant, the KPZ field theory description breaks down and the entanglement deviates from the predicted value based on the $q^{-1/3}$ scaling. The choice of boundary condition does not change the entanglement behaviors qualitatively (see the numerical results with open bo undary condition (OBC) in Ref. [56]). The entanglement with PBC is about twice as large as that with OBC in the noise-driven area law phase.

Effective statistical model. The numerical results in this Letter can be well explained by a mapping to an effective statistical model. We build upon the previous works [52] for a unified analytical picture to understand the noise effects in the monitored random circuit.

To compute the entanglement from the effective statistical model, we consider the nth Rényi entropy $S_\alpha^{(n)}$ first. For fixed sets of measurement locations X and reset locations Y in the circuit, averaged over Haar unitary $U = \{U_{ij,t}\}$ and measurement results m, $S_\alpha^{(n)}$ is

$$\overline{S_\alpha^{(n)}(X,Y)} = \mathbb{E}_U \sum_m p_{m,X,Y} \frac{1}{1-n} \log\left\{\frac{\mathrm{tr}\left(\rho_{\alpha,m,X,Y}^n\right)}{(\mathrm{tr}\rho_{m,X,Y})^n}\right\}, \quad (4)$$

where α denotes the subsystem ($\alpha = A, B, AB$), $\rho_{m,X,Y}$ is the un-normalized density matrix given the measurement trajectory m, with probability $p_{m,X,Y} = \mathrm{tr}\rho_{m,X,Y}$.

The average of the logarithmic function can be evaluated via the replica trick [73,74]. To this end, we first perform the average over unitary realizations inside the logarithmic function,

$$\begin{aligned} S_\alpha^{(n,k)} &= \frac{1}{k(1-n)} \log\left\{\frac{Z_{S_\alpha}^{(n,k)}}{Z^{(n,k)}}\right\}, \\ &= \frac{1}{k(n-1)}\left(F_{S_\alpha}^{(n,k)} - F^{(n,k)}\right). \end{aligned} \quad (5)$$

We map the $1+1$ dimensional hybrid circuit with replica trick to a two-dimensional effective statistical model with classical spin freedom that is valued over permutation group S_{nk+1} with the ferromagnetic spin-spin interaction [56]. Z's are the partition functions of the statistical models with different top boundary conditions: $Z^{(n,k)}$ contains identity permutations $\mathbb{I}$ along the entire top boundary whereas $Z_{S_\alpha}^{(n,k)}$ contains cyclic permutation $\mathbb{C}$ at the top region α and identity permutation $\mathbb{I}$ at the top complementary region (see Fig. 3). The mutual information is the difference of free energies F of statistical models with specific boundary conditions,

$$\begin{aligned} I_{A:B} &= \lim_{\substack{n\to 1\\ k\to 0}} \left(S_A^{(n,k)} + S_B^{(n,k)} - S_{AB}^{(n,k)}\right), \\ &= \lim_{\substack{n\to 1\\ k\to 0}} \frac{1}{k(n-1)}\left(F_{S_A}^{(n,k)} + F_{S_B}^{(n,k)} - F_{S_{AB}}^{(n,k)}\right). \end{aligned} \quad (6)$$

The logarithmic entanglement negativity can also be obtained from the replica negativity similarly, which we defer the derivation in Ref. [56].

In the large $d \to \infty$ limit, the free energy of the effective statistical model is determined by the most probable classical spin configuration and proportional to the domain-wall length due to the ferromagnetic spin-spin interaction. In the absence of measurements and resets, the domain wall is unique for the statistical model with specific boundary conditions due to the unitary constraint, and the length is proportional to L. The measurements act as the pointwise attractive potential, and the randomness of measurement locations can be regarded as the quenched disorders. In the coarse-grained picture, the effective statistical model is equivalent to the model of directed polymers in a random Gaussian potential described by the KPZ field theory [52,67–69]. Thus, the directed polymer, i.e., the domain wall, in the randomly monitored measurement background, fluctuates slightly away from the unique trajectory. The length and length scale of the vertical fluctuations of the domain wall are, thus, $s_0 L + s_1 L^{1/3}$ and $O(L^{2/3})$, respectively.

The reset quantum channels in the bulk act as a symmetry-breaking field after mapping to the statistical model, and the free energy is minimized when the classical spin permutation freedom is pinned to identity $\mathbb{I}$. Due to the nonidentity spin permutation freedom induced by the top boundary α, the free-energy cost is proportional to the number of the resets contained between the domain wall and the top boundary α. To avoid this cost, the length scale of vertical fluctuations of the domain wall can be suppressed to exclude more resets. Equivalently, the resets in the bulk can be interpreted as attractive potential from the top boundary and can induce the pinning phase transition where the $O(L^{2/3})$ KPZ vertical fluctuations with length scale L vanishes, and the system enters the pinned phases, i.e., area law entanglement phase [75,76]. Besides, the resets near the top boundary can further induce an effective length scale $L_{\mathrm{eff}} \sim q^{-1}$ (on average, the distance between two adjoint reset channels in the same layer is q^{-1}) and open a possible way for the directed polymer to fluctuate vertically with the emergent and smaller length scale L_{eff} as indicated in Fig. 3. And the domain-wall length is now $s_0 L_{\mathrm{eff}} + s_1 L_{\mathrm{eff}}^{1/3}$ due to the KPZ fluctuation [52,67–69].

The two possible scenarios discussed above are summarized in Fig. 3 where we assume OBC for simplicity. For $Z_{S_{AB}}^{(n,k)}$, if the two end points of the directed polymer are in the same region (A or B), the free-energy contribution is canceled by the directed polymer in $Z_{S_A}^{(n,k)}$ or $Z_{S_B}^{(n,k)}$, and the contribution to the mutual information is zero; if the two end points are in the regions A and B, respectively, as the middle directed polymer shown in Fig. 3(c), the contribution to the mutual information is proportional to $L_{\mathrm{eff}}^{1/3} \sim q^{-1/3}$ [52,56]. Therefore, the novel power-law scaling in terms of reset probability q shown in Fig. 2 can be understood as the consequence of the KPZ fluctuation with an emergent effective length scale $L_{\mathrm{eff}} \sim q^{-1}$. And it is straightforward that the entanglement with PBC is twice as the OBC case because the directed polymer can cross the side boundary as well as the middle point, which has a nonzero contribution to the mutual information. In the absence of monitored measurements, i.e., the random attractive potential, the $q^{-1/3}$ scaling disappears [56].

To further verify the statistic model mapping and the analytic picture, we consider another model in which there are resets on the spatial boundary of the hybrid circuit and random bulk resets only on the last t_{noise} layers as shown in Fig. 1(b). This model is the same as Ref. [52] with the $q = 0$ limit or

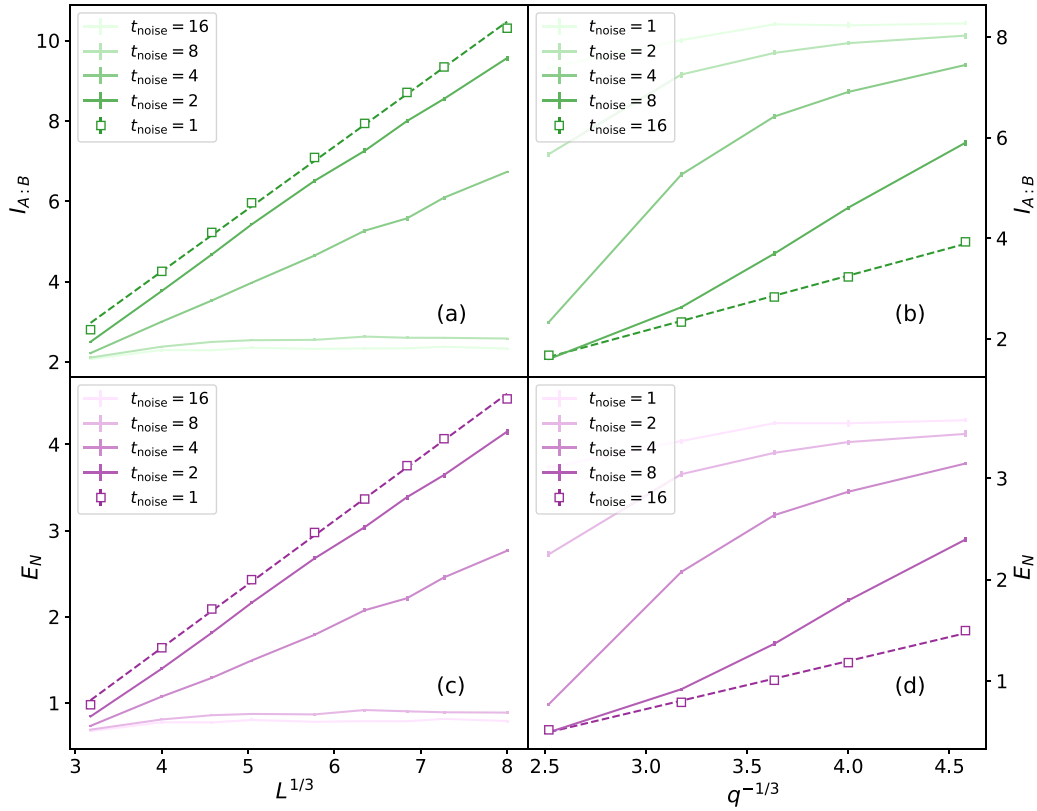

FIG. 4. (a) $I_{A:B}$ and (c) E_N with fixed $q = 1/32$ and different t_{noise}'s. When t_{noise} is small, the quantum noise is not enough to suppress the $L^{1/3}$ entanglement by inducing the pinning phase transition, and the $L^{1/3}$ scaling still exists; when t_{noise} is large, the system enters the area law entanglement phase. (b) $I_{A:B}$ and (d) E_N with fixed system size $L = 256$ and different t_{noise}'s. When t_{noise} is large, the volume law entanglement vanishes and the $q^{-1/3}$ scaling appears.

the $t_{\text{noise}} = 0$ limit (with dephasing channel replaced by the reset channel). In the $t_{\text{noise}} \to \infty$ limit, this model is the same as that shown in Fig. 1(a) with rescaled p and q. Based on the analytic picture discussed above, the resets occurring at a small rate q are not enough to suppress the $O(L^{2/3})$ vertical fluctuations, and the systems exhibit the power-law scaling $(L^{1/3})$ entanglement when t_{noise} is small. With increasing the t_{noise}, the $O(L^{2/3})$ vertical fluctuation vanishes, and the system enters the area law entanglement phase with a novel power-law scaling $q^{-1/3}$ as indicated in Fig. 4. Interpolated by this model, the boundary quantum noise and the bulk quantum noise are unified. In terms of the statistical model, they both play a role in fixing the end points of the directed polymer and, thus, induce length scales $O(L)$ and $O(q^{-1})$, respectively.

Another strategy to detect this entanglement phase transition and verify the analytic picture is by increasing q with fixed t_{noise}, similar to the pinned phase-transition setup investigated in Ref. [76]. This approach has also been studied and can be found in Ref. [56].

Conclusions and discussions. To conclude, we show that the reset quantum channel in the bulk can drive the systems to enter the area law entanglement phase as a consequence of the symmetry breaking in the effective statistical model. More importantly, we identify a novel power-law scaling $(q^{-1/3})$ in the quantum noise-driven area law phase as the result of KPZ fluctuations with an effective length scale $L_{\text{eff}} \sim q^{-1}$. This new analytic picture, supported by convincing numerical results from models with different space-time distributions of quantum noises, unifies the understanding of boundary and bulk quantum noise in which the difference is the effective length scale induced by the distribution of quantum noise. Our results and understanding are also crucial for any experimental implementation of the MIPT system in the noisy intermediate-scale quantum devices.

Since all decoherence quantum channels break the permutation symmetry in the effective statistical model, the novel power-law scaling $(q^{-1/3})$ remains in the presence of other quantum noises as a universal behavior in noisy hybrid circuits. Moreover, as indicated by the $q^{-1/3}$ scaling, an interesting future direction is to investigate whether we can identify nontrivial entanglement structure using local probes even in the noise-driven area law phase.

Acknowledgements. This work was supported, in part, by the CAS Strategic Priority Research Program under Grant No. XDB28000000 (H.Y.), the NSFC under Grant No. 11825404 (S.L., M.-R.L., and H.Y.), and the MOSTC Grant No. 2021YFA1400100 (H.Y.). S.-K.J. was supported by a startup fund at Tulane University.

[1] Y. Li, X. Chen, and M. P. A. Fisher, Quantum zeno effect and the many-body entanglement transition, Phys. Rev. B **98**, 205136 (2018).

[2] Y. Li, X. Chen, and M. P. A. Fisher, Measurement-driven entanglement transition in hybrid quantum circuits, Phys. Rev. B **100**, 134306 (2019).

[3] B. Skinner, J. Ruhman, and A. Nahum, Measurement-Induced Phase Transitions in the Dynamics of Entanglement, Phys. Rev. X **9**, 031009 (2019).

[4] M. Ippoliti and V. Khemani, Postselection-Free Entanglement Dynamics via Spacetime Duality, Phys. Rev. Lett. **126**, 060501 (2021).

[5] M. Ippoliti, T. Rakovszky, and V. Khemani, Fractal, Logarithmic, and Volume-Law Entangled Nonthermal Steady States via Spacetime Duality, Phys. Rev. X **12**, 011045 (2022).

[6] T.-C. Lu and T. Grover, Spacetime duality between localization transitions and measurement-induced transitions, PRX Quantum **2**, 040319 (2021).

[7] S. Choi, Y. Bao, X.-L. Qi, and E. Altman, Quantum Error Correction in Scrambling Dynamics and Measurement-Induced Phase Transition, Phys. Rev. Lett. **125**, 030505 (2020).

[8] M. J. Gullans and D. A. Huse, Dynamical Purification Phase Transition Induced by Quantum Measurements, Phys. Rev. X **10**, 041020 (2020).

[9] A. Chan, R. M. Nandkishore, M. Pretko, and G. Smith, Unitary-projective entanglement dynamics, Phys. Rev. B **99**, 224307 (2019).

[10] M. Szyniszewski, A. Romito, and H. Schomerus, Entanglement transition from variable-strength weak measurements, Phys. Rev. B **100**, 064204 (2019).

[11] Y. Bao, S. Choi, and E. Altman, Theory of the phase transition in random unitary circuits with measurements, Phys. Rev. B **101**, 104301 (2020).

[12] R. Fan, S. Vijay, A. Vishwanath, and Y.-Z. You, Self-organized error correction in random unitary circuits with measurement, Phys. Rev. B **103**, 174309 (2021).

[13] Y. Li and M. P. A. Fisher, Statistical mechanics of quantum error correcting codes, Phys. Rev. B **103**, 104306 (2021).

[14] C.-M. Jian, Y.-Z. You, R. Vasseur, and A. W. W. Ludwig, Measurement-induced criticality in random quantum circuits, Phys. Rev. B **101**, 104302 (2020).

[15] S. Sahu, S.-K. Jian, G. Bentsen, and B. Swingle, Entanglement phases in large-N hybrid Brownian circuits with long-range couplings, Phys. Rev. B **106**, 224305 (2022).

[16] S.-K. Jian and B. Swingle, Phase transition in von Neumann entanglement entropy from replica symmetry breaking, arXiv:2108.11973.

[17] S.-K. Jian, C. Liu, X. Chen, B. Swingle, and P. Zhang, Measurement-Induced Phase Transition in the Monitored Sachdev-ye-Kitaev Model, Phys. Rev. Lett. **127**, 140601 (2021).

[18] T. Jin and D. G. Martin, Kardar-Parisi-Zhang Physics and Phase Transition in a Classical Single Random Walker under Continuous Measurement, Phys. Rev. Lett. **129**, 260603 (2022).

[19] P. Sierant, G. Chiriacò, F. M. Surace, S. Sharma, X. Turkeshi, M. Dalmonte, R. Fazio, and G. Pagano, Dissipative floquet dynamics: From steady state to measurement induced criticality in trapped-ion chains, Quantum **6**, 638 (2022).

[20] A. Nahum, S. Roy, B. Skinner, and J. Ruhman, Measurement and entanglement phase transitions in all-to-all quantum circuits, on quantum trees, and in landau-ginsburg theory, PRX Quantum **2**, 010352 (2021).

[21] G. S. Bentsen, S. Sahu, and B. Swingle, Measurement-induced purification in large-n hybrid brownian circuits, Phys. Rev. B **104**, 094304 (2021).

[22] X. Yu and X.-L. Qi, Measurement-induced entanglement phase transition in random bilocal circuits, arXiv:2201.12704.

[23] S. Vijay, Measurement-driven phase transition within a volume-law entangled phase, arXiv:2201.12704.

[24] T. Müller, S. Diehl, and M. Buchhold, Measurement-Induced Dark State Phase Transitions in Long-Ranged Fermion Systems, Phys. Rev. Lett. **128**, 010605 (2022).

[25] M. Block, Y. Bao, S. Choi, E. Altman, and N. Y. Yao, Measurement-Induced Transition in Long-Range Interacting Quantum Circuits, Phys. Rev. Lett. **128**, 010604 (2022).

[26] T. Hashizume, G. Bentsen, and A. J. Daley, Measurement-induced phase transitions in sparse nonlocal scramblers, Phys. Rev. Res. **4**, 013174 (2022).

[27] T. Minato, K. Sugimoto, T. Kuwahara, and K. Saito, Fate of Measurement-Induced Phase Transition in Long-Range Interactions, Phys. Rev. Lett. **128**, 010603 (2022).

[28] S. Sharma, X. Turkeshi, R. Fazio, and M. Dalmonte, Measurement-induced criticality in extended and long-range unitary circuits, SciPost Phys. Core **5**, 023 (2022).

[29] C. H. Bennett, D. P. DiVincenzo, J. A. Smolin, and W. K. Wootters, Mixed-state entanglement and quantum error correction, Phys. Rev. A **54**, 3824 (1996).

[30] M. Horodecki, P. Horodecki, and R. Horodecki, Mixed-State Entanglement and Distillation: Is There a "bound" Entanglement in Nature? Phys. Rev. Lett. **80**, 5239 (1998).

[31] G. Vidal and R. F. Werner, Computable measure of entanglement, Phys. Rev. A **65**, 032314 (2002).

[32] M. B. Plenio, Logarithmic Negativity: A Full Entanglement Monotone that is not Convex, Phys. Rev. Lett. **95**, 090503 (2005).

[33] P. Calabrese, J. Cardy, and E. Tonni, Entanglement Negativity in Quantum Field Theory, Phys. Rev. Lett. **109**, 130502 (2012).

[34] P. Calabrese, J. Cardy, and E. Tonni, Entanglement negativity in extended systems: a field theoretical approach, J. Stat. Mech.: Theory Exp. (2013) P02008.

[35] T.-C. Lu and T. Grover, Singularity in entanglement negativity across finite-temperature phase transitions, Phys. Rev. B **99**, 075157 (2019).

[36] T.-C. Lu, T. H. Hsieh, and T. Grover, Detecting Topological Order at Finite Temperature using Entanglement Negativity, Phys. Rev. Lett. **125**, 116801 (2020).

[37] K.-H. Wu, T.-C. Lu, C.-M. Chung, Y.-J. Kao, and T. Grover, Entanglement Renyi Negativity across a Finite Temperature Transition: A Monte Carlo Study, Phys. Rev. Lett. **125**, 140603 (2020).

[38] T.-C. Lu and T. Grover, Entanglement transitions as a probe of quasiparticles and quantum thermalization, Phys. Rev. B **102**, 235110 (2020).

[39] S. Sang, Y. Li, T. Zhou, X. Chen, T. H. Hsieh, and M. P. Fisher, Entanglement negativity at measurement-induced criticality, PRX Quantum **2**, 030313 (2021).

[40] H. Shapourian, S. Liu, J. Kudler-Flam, and A. Vishwanath, Entanglement negativity spectrum of random mixed states: A diagrammatic approach, PRX Quantum **2**, 030347 (2021).

[41] X. Turkeshi, L. Piroli, and M. Schiró, Enhanced entanglement negativity in boundary-driven monitored fermionic chains, Phys. Rev. B **106**, 024304 (2022).

[42] H. Kim and D. A. Huse, Ballistic Spreading of Entanglement in a Diffusive Nonintegrable System, Phys. Rev. Lett. **111**, 127205 (2013).

[43] A. M. Kaufman, M. E. Tai, A. Lukin, M. Rispoli, R. Schittko, P. M. Preiss, and M. Greiner, Quantum thermalization through entanglement in an isolated many-body system, Science **353**, 794 (2016).

[44] A. Nahum, J. Ruhman, S. Vijay, and J. Haah, Quantum Entanglement Growth under Random Unitary Dynamics, Phys. Rev. X **7**, 031016 (2017).

[45] F. Arute, K. Arya, R. Babbush, D. Bacon, J. C. Bardin, R. Barends, R. Biswas, S. Boixo, F. G. S. L. Brandao, D. A. Buell, B. Burkett, Y. Chen, Z. Chen, B. Chiaro, R. Collins, W. Courtney, A. Dunsworth, E. Farhi, B. Foxen, A. Fowler, C. Gidney, M. Giustina, R. Graff, K. Guerin, S. Habegger, M. P. Harrigan, M. J. Hartmann, A. Ho, M. Hoffmann, T. Huang, T. S. Humble, S. V. Isakov, E. Jeffrey, Z. Jiang, D. Kafri, K. Kechedzhi, J. Kelly, P. V. Klimov, S. Knysh, A. Korotkov, F. Kostritsa, D. Landhuis, M. Lindmark, E. Lucero, D. Lyakh, S. Mandrà, J. R. McClean, M. McEwen, A. Megrant, X. Mi, K. Michielsen, M. Mohseni, J. Mutus, O. Naaman, M. Neeley, C. Neill, M. Y. Niu, E. Ostby, A. Petukhov, J. C. Platt, C. Quintana, E. G. Rieffel, P. Roushan, N. C. Rubin, D. Sank, K. J. Satzinger, V. Smelyanskiy, K. J. Sung, M. D. Trevithick, A. Vainsencher, B. Villalonga, T. White, Z. J. Yao, P. Yeh, A. Zalcman, H. Neven, and J. M. Martinis, Quantum supremacy using a programmable superconducting processor, Nature (London) **574**, 505 (2019).

[46] J. Choi, A. L. Shaw, I. S. Madjarov, X. Xie, R. Finkelstein, J. P. Covey, J. S. Cotler, D. K. Mark, H.-Y. Huang, A. Kale, H. Pichler, F. G. S. L. Brandão, S. Choi, and M. Endres, Emergent quantum randomness and benchmarking from hamiltonian many-body dynamics, Nature (London) **613**, 468 (2023).

[47] C. Noel, P. Niroula, D. Zhu, A. Risinger, L. Egan, D. Biswas, M. Cetina, A. V. Gorshkov, M. J. Gullans, D. A. Huse, and C. Monroe, Measurement-induced quantum phases realized in a trapped-ion quantum computer, Nat. Phys. **18**, 760 (2022).

[48] M. Ippoliti, M. J. Gullans, S. Gopalakrishnan, D. A. Huse, and V. Khemani, Entanglement Phase Transitions in Measurement-Only Dynamics, Phys. Rev. X **11**, 011030 (2021).

[49] Y. Bao, S. Choi, and E. Altman, Symmetry enriched phases of quantum circuits, Ann. Phys. (Amsterdam) **435**, 168618 (2021).

[50] B. C. Dias, D. Perkovic, M. Haque, P. Ribeiro, and P. A. McClarty, Quantum noise as a symmetry-breaking field, arXiv:2208.13861.

[51] S.-K. Jian, C. Liu, X. Chen, B. Swingle, and P. Zhang, Quantum error as an emergent magnetic field, arXiv:2106.09635.

[52] Z. Weinstein, Y. Bao, and E. Altman, Measurement-Induced Power-Law Negativity in an Open Monitored Quantum Circuit, Phys. Rev. Lett. **129**, 080501 (2022).

[53] J. C. Hoke, M. Ippoliti, D. Abanin, R. Acharya, M. Ansmann, F. Arute, K. Arya, A. Asfaw, J. Atalaya, J. C. Bardin, A. Bengtsson, G. Bortoli, A. Bourassa, J. Bovaird, L. Brill, M. Broughton, B. B. Buckley, D. A. Buell, T. Burger, B. Burkett, N. Bushnell, Z. Chen, B. Chiaro, D. Chik, C. Chou, J. Cogan, R. Collins, P. Conner, W. Courtney, A. L. Crook, B. Curtin, A. G. Dau, D. M. Debroy, A. D. T. Barba, S. Demura, A. Di Paolo, I. K. Drozdov, A. Dunsworth, D. Eppens, C. Erickson, L. Faoro, E. Farhi, R. Fatem, V. S. Ferreira, L. F. Burgos, E. Forati, A. G. Fowler, B. Foxen, W. Giang, C. Gidney, D. Gilboa, M. Giustina, R. Gosula, J. A. Gross, S. Habegger, M. C. Hamilton, M. Hansen, M. P. Harrigan, S. D. Harrington, P. Heu, M. R. Hoffmann, S. Hong, T. Huang, A. Huff, W. J. Huggins, S. V. Isakov, J. Iveland, E. Jeffr, C. Jones, P. Juhas, D. Kafri, K. Kechedzhi, T. Khattar, M. Khezri, M. Kieferová, S. Kim, A. Kitaev, P. V. Klimov, A. R. Klots, A. N. Korotkov, F. Kostritsa, J. M. Kreikebaum, D. Landhuis, P. Laptev, K.-M. Lau, L. Laws, J. Lee, K. W. Lee, Y. D. Lensky, B. J. Lester, A. T. Lill, W. Liu, A. Locharla, F. D. Malone, O. Martin, J. R. McClean, T. McCourt, M. McEwen, K. C. Miao, A. Mieszala, S. Montazeri, A. Morvan, R. Movassagh, W. Mruczkiewicz, M. Neeley, C. Neill, A. Nersisyan, M. Newman, J. H. Ng, A. Nguyen, M. Nguyen, M. Y. Niu, T. E. O'Brien, S. Omonije, A. Opremcak, A. Petukhov, R. Potter, L. P. Pryadko, C. Quintana, C. Rocque, N. C. Rubin, N. S. D. Sank, K. Sankaragomathi, K. J. Satzinger, H. F. Schurkus, C. Schuster, M. J. Shearn, A. Shorter, N. Shutty, V. Shvarts, J. Skruzny, W. C. Smith, R. D. S. G. Sterling, D. Strain, M. Szalay, A. Torres, G. Vidal, B. Villalonga, C. V. Heidweiller, T. White, B. W. K. Woo, C. Xing, Z. J. Yao, P. Yeh, J. Yoo, G. Young, A. Zalcman, Y. Zhang, N. Zhu, N. Zobrist, H. Neven, R. Babbush, D. Bacon, S. Boixo, J. Hilton, E. Lucero, A. Megrant, J. Kelly, Y. Chen, V. Smelyanskiy, X. Mi, V. Khemani, and P. Roushan, Quantum information phases in space-time: Measurement-induced entanglement and teleportation on a noisy quantum processor, arXiv:2303.04792.

[54] Y. Zhou, Z. Zhang, Z. Yin, S. Huai, X. Gu, X. Xu, J. Allcock, F. Liu, G. Xi, Q. Yu, H. Zhang, M. Zhang, H. Li, X. Song, Z. Wang, D. Zheng, S. An, Y. Zheng, and S. Zhang, Rapid and unconditional parametric reset protocol for tunable superconducting qubits, Nat. Commun. **12**, 5924 (2021).

[55] K. Geerlings, Z. Leghtas, I. M. Pop, S. Shankar, L. Frunzio, R. J. Schoelkopf, M. Mirrahimi, and M. H. Devoret, Demonstrating a Driven reset Protocol for a Superconducting Qubit, Phys. Rev. Lett. **110**, 120501 (2013).

[56] See Supplemental Material at http://link.aps.org/supplemental/10.1103/PhysRevB.107.L201113 for details, including the following: (1) the results with open boundary condition, (2) the results with large measurement rate $p > p_c$, (3) the results with zero measurement rate $p = 0$, (4) the comparison of different fitting functions, (5) pinned phase via increasing the reset occurring rate q, (6) the details of Clifford simulation, (7) effective statistical model, and Refs. [57–66].

[57] D. Gottesman, The Heisenberg Representation of Quantum Computers, arXiv:quant-ph/9807006.

[58] S. Aaronson and D. Gottesman, Improved simulation of stabilizer circuits, Phys. Rev. A **70**, 052328 (2004).

[59] M. A. Nielsen, I. Chuang, and L. K. Grover, Quantum Computation and Quantum Information, Am. J. Phys. **70**, 558 (2002).

[60] B. Shi, X. Dai, and Y.-M. Lu, Entanglement negativity at the critical point of measurement-driven transition, arXiv:2012.00040.

[61] T. Zhou and A. Nahum, Emergent statistical mechanics of entanglement in random unitary circuits, Phys. Rev. B **99**, 174205 (2019).

[62] U. Agrawal, A. Zabalo, K. Chen, J. H. Wilson, A. C. Potter, J. H. Pixley, S. Gopalakrishnan, and R. Vasseur, Entanglement and Charge-Sharpening Transitions in U(1) Symmetric Monitored Quantum Circuits, Phys. Rev. X **12**, 041002 (2022).

[63] B. Collins, Moments and cumulants of polynomial random variables on unitarygroups, the itzykson-zuber integral, and free probability, Int. Math. Res. Not. **2003**, 953 (2003).

[64] B. Collins and P. Śniady, Integration with respect to the Haar measure on unitary, orthogonal and symplectic group, Commun. Math. Phys. **264**, 773 (2006).

[65] A. Nahum, S. Vijay, and J. Haah, Operator Spreading in Random Unitary Circuits, Phys. Rev. X **8**, 021014 (2018).

[66] J. Quastel and H. Spohn, The one-dimensional KPZ equation and its universality class, J. Stat. Phys. **160**, 965 (2015).

[67] M. Kardar, G. Parisi, and Y.-C. Zhang, Dynamic Scaling of Growing Interfaces, Phys. Rev. Lett. **56**, 889 (1986).

[68] M. Kardar, Roughening by Impurities at Finite Temperatures, Phys. Rev. Lett. **55**, 2923 (1985).

[69] D. A. Huse, C. L. Henley, and D. S. Fisher, Huse, Henley, and Fisher Respond, Phys. Rev. Lett. **55**, 2924 (1985).

[70] Z. Webb, The Clifford group forms a unitary 3-design, Quantum Inf. Comput. **16**, 1379 (2016).

[71] E. van den Berg, A simple method for sampling random Clifford operators, *2021 IEEE International Conference on Quantum Computing and Engineering (QCE)* (Broomfield, CO, USA, 2021), pp. 54–59.

[72] T. Boorman, M. Szyniszewski, H. Schomerus, and A. Romito, Diagnostics of entanglement dynamics in noisy and disordered spin chains via the measurement-induced steady-state entanglement transition, Phys. Rev. B **105**, 144202 (2022).

[73] M. Kardar, *Statistical Physics of Fields* (Cambridge University Press, Cambridge, UK, 2007).

[74] H. Nishimori, *Statistical Physics of Spin Glasses and Information Processing: An Introduction* (Oxford University Press, Oxford, 2001).

[75] M. Kardar, Depinning by Quenched Randomness, Phys. Rev. Lett. **55**, 2235 (1985).

[76] Y. Li, S. Vijay, and M. P. A. Fisher, Entanglement domain walls in monitored quantum circuits and the directed polymer in a random environment, PRX Quantum **4**, 010331 (2023).